

A Theoretical Study on the Benefits of Integrating GNSS and Collaborative Relative Ranges

Original

A Theoretical Study on the Benefits of Integrating GNSS and Collaborative Relative Ranges / Minetto, Alex. - ELETTRONICO. - (2019), pp. 1951-1962. (Intervento presentato al convegno 32nd International Technical Meeting of The Satellite Division of the Institute of Navigation (ION GNSS+ 2019) tenutosi a Hyatt Regency Hotel, Miami (FL) nel Sept. 16-20, 2019) [10.33012/2019.16877].

Availability:

This version is available at: 11583/2759516 since: 2019-12-19T10:00:02Z

Publisher:

The Institute of Navigation, Inc.

Published

DOI:10.33012/2019.16877

Terms of use:

This article is made available under terms and conditions as specified in the corresponding bibliographic description in the repository

Publisher copyright

(Article begins on next page)

A Theoretical Study on the Benefits of Integrating GNSS and Collaborative Relative Ranges

Alex Minetto, *IEEE, Student Member*

Alex Minetto received the M.Sc. in telecommunications engineering (Information Theory and Signal Processing Applications) from Politecnico di Torino, Italy, in 2015. He is currently a PhD candidate at the Department of Electronics and Telecommunications of Politecnico di Torino within the Navigation Signal Analysis and Simulation (NavSAS) research group. He was an intern at the European Organization for the Exploitation of Meteorological Satellites (EUMETSAT) in Darmstadt (Germany), addressing the development of a new precise detection algorithm for radar pulses sent from Metop satellites during their calibration campaign. His research interests include information theory, advanced signal processing, Global Navigation Satellite System (GNSS), and collaborative positioning.

Abstract

Previous research contributions addressed the definition of a Cramer Rao Lower Bound (CRLB) as a theoretical tool to investigate the performance of unbiased position estimators for deterministic non linear systems. Moving from such theoretical findings, this work aims at investigating the CRLB of hybrid estimators integrating auxiliary measurements obtained from the combination of satellite-based range measurements shared among pairs of connected receivers. The study is conceived to inspect the benefits of this GNSS-based collaborative positioning approach in terms of precision improvement. The analysis of such a theoretical limit aims at identifying when the use of cooperative ranges is beneficial despite of their correlation with the individual measurements, according to the geometry of satellites and terrestrial agents w.r.t. a target agent. The theoretical analysis is validated by simulation by demonstrating when the collaborative measurements increases the precision of the position estimates. The study practically provides a methodology for the selection of the best cooperating agents in multi-agent frameworks.

Index Terms

Cramer Rao bound, Satellite navigation systems, Cooperative systems, Position estimation

I. INTRODUCTION

Positioning accuracy and precision have always been of the utmost importance in a wide range of location-based services and applications. To satisfy such increasing requirements, in the last decade, aided positioning first and then cooperative positioning have gained relevance in compensating the weaknesses of Global Satellite Navigation System (GNSS) and increasing the performance. In parallel with the integration of inertial sensors and vision-based systems, cooperative solutions can exploit connected terrestrial agents to retrieve additional exteroceptive information from the neighbours [?]. Several techniques showed that the estimation of the GNSS positioning solution can be improved by merging different range information from auxiliary reference landmarks such as base stations, beacons and peer agents. Theoretical limits of cooperative positioning have been investigated in several works by mainly considering independent measurement contributions that are merged with the GNSS measurements in the positioning estimation. For example, in [?] the author first investigate the problem in the framework of sensor networks, in [?], [?] an exhaustive theoretical analysis on the topic is provided for cooperative networks applications and in [?] the authors have derived the Cramer Rao Lower Bound (CRLB) for localization and navigation by means of generic hybrid cooperative solutions. The measurements have been typically assumed to be statistically independent and Gaussian distributed such that their uncorrelation has been assessed by definition [?]. As a consequence, it has been shown that under these assumption the overall quantity of information carried by the measurements is simply the sum of the independent information contributions.

Despite such cooperative approaches are known to be intuitively beneficial against impairments and to generally improve accuracy, few contributions exploited the idea of collaborative determination of inter agent ranges as a potential source of information to the positioning problem [?], [?], [?]. An evidence in showing that the combination of satellite and correlated terrestrial measurements can still bring benefits in terms of quantity of information is missing in literature. To the purpose, a relevant contribution have been proposed about the formulation of a Collaborative Dilution of Precision (CDOP) [?], and a theoretical performance analysis about basic collaborative navigation has been presented in [?].

The main challenge in this analysis is that the use of measurements such as GNSS-based ranging introduces correlation within the set of measurements involved in the positioning problem, thus weakening the conditions typically assumed for the computation of theoretical limits (i.e. statistical independence, known probability distribution). Such a correlation is either due to the use of the estimated position itself or the use of combined pseudorange measurements as exploited in several ranging algorithms (see for example [?], [?]). Furthermore, the statistical properties of such kind of measurements are not well-defined in literature due to their strong dependency on the geometrical configuration and the features of the investigated scenario. Previous analyses supported that the identification of clear advantages of this integration is challenging due to the aforementioned properties of the measurements [?]. Despite these drawbacks, numerical experiments performed in a more controlled simulation environment returned remarkable improvements of the hybrid solution w.r.t. the plain GNSS, mostly in terms of precision. This evidence pushed the need of the theoretical analysis which is presented in this work.

When the minimum number of reference landmarks (and relative measurements) is exceeded, a selection of the information sources can be applied to improve the positioning performance. As observed in [?] indeed, the integration of additional measurements could even deteriorate the performance. Indeed, previous works partially addressed the *source censoring* by minimizing the Cramer Rao Lower Bound (CRLB) within the framework of wireless sensor networks [?], [?], [?]. The metric considered in this work is derived from an approximation of the CRLB to estimate the covariance of a hybrid Least Mean Square (H-LMS) and hybrid Extended Kalman Filter (H-EKF) position estimators based on correlated input measurements. The metric is hence conceived to flag the effectiveness of the integration of collaborative ranging measurements especially for LMS estimation for which, differently from EKF, the advantage of the integration is not always evident neither present.

The paper is organized as follows: Section II illustrates the modelling of the involved measurements; Section III recalls the derivation of the Fisher Information Matrix for the position estimation computed through LMS and EKF algorithms; Section V describe the simulation environment and the metrics. Eventually, section VI discusses numerical results obtained through meaningful dynamic examples for the two estimators when they are applied to the positioning problem on a set of simple geometrical trajectories.

II. BACKGROUND

The amount of information carried by any unbiased range measurements w.r.t. to the current position is related to the quality of the observable measurements and to the relative position of the involved reference points [?]. On one hand, the goodness of this information is inversely proportional to the variance of the measurement error itself. On the other hand, the direction w.r.t. each range is obtained leads to a fundamental issue known as Geometrical Dilution Of Precision (GDOP). The GDOP affects the positioning solutions by directly altering the covariance of their statistical distribution [?], namely its precision. The combination of these two factors characterize the positioning error, derived as in [?] from the Cramer Rao Lower Bound of the positioning estimator. A minimization of the GDOP can be applied in GNSS to select the best set of satellites and a generalized CRLB-based approach is proposed in the following for hybrid positioning including both satellites and GNSS-based terrestrial measurements.

A. The Fisher Information and the Cramer Rao Lower Bound

The CRLB is employed to identify the minimum variance that can be reached by a given unbiased estimator [?] according to the statistics of the observable measurements. Indeed, the related Cramer Rao inequality states that this variance is bounded by the inverse of the *Fisher Information* carried by the observable set of measurements. This fundamental limit can be generalized in its matrix form, as

$$[P_{\theta}]_{i,j} \geq [F_{\theta}]_{i,j}^{-1} = \left[-\mathbf{E} \left(\frac{\partial^2}{\partial \theta_i \partial \theta_j} \log f(\boldsymbol{\mu}; \boldsymbol{\theta}) \Big|_{\boldsymbol{\theta}} \right) \right]^{-1} \quad (1)$$

where $\boldsymbol{\theta} = [\theta_1, \theta_2, \dots, \theta_M]^T$ is a $M \times 1$ vector which defines the *target state* and $\boldsymbol{\theta}$ is the associated estimator, $\boldsymbol{\mu}$ is the observed realization of a multivariate *measurements vector* which is associated to $\boldsymbol{\theta}$ by means of the probability density function $f(\boldsymbol{\mu}; \boldsymbol{\theta})$. The subscripts i, j indicate the i -th row and j -th column of the matrix elements, respectively while F_{θ} is a $M \times M$ matrix named *Fisher Information Matrix* (FIM) whose inverse is namely the CRLB.

Given that both $P_{\hat{\theta}}$ and $[F_{\theta}]^{-1}$ are positive definite, an ordering relation can be defined to compare two estimators identified as $T(\boldsymbol{\theta})$ and $T'(\boldsymbol{\theta})$, according to

$$[F_{T,\boldsymbol{\theta}}]^{-1} > [F_{T',\boldsymbol{\theta}}]^{-1} \iff \text{Tr}([F_{T,\boldsymbol{\theta}}]^{-1}) > \text{Tr}([F_{T',\boldsymbol{\theta}}]^{-1}) \quad (2)$$

where $\text{Tr}(\cdot)$ is the trace operator defined as the sum of the diagonal terms of the argument. Whether unbiased estimators are considered, the comparison of the respective CRLBs (1) allows to identify which estimation provides more information about

the value of interest. This study presents the comparison of GNSS-only and hybrid positioning computation and shows that a terrestrial correlated range brings information to the position estimation process according to the values assumed by the related CRLB.

B. Range measurements modelling

In this study, two classes of range measurements are identified as observable random variables composing the *measurements vector* in (1). They are introduced through their conventional model by assuming independence and Gaussian distribution in order to support the following computation steps. All the models are defined w.r.t. the generic *target agent*, m :

- $\hat{\rho}_{s,m}(t_k)$ is an estimate of the *pseudorange* between agent m and satellite s at a given instant t_k [?], defined as

$$\hat{\rho}_{s,m}(t_k) = \|\mathbf{x}_s(t_k) - \mathbf{x}_m(t_k)\| + b_m(t_k) + \nu_{s,m}(t_k) \quad (3)$$

where $b_m(t_k)$ is a bias term due to the clocks misalignment and $\nu_{s,m}(t_k)$ is the noise due to residual errors affecting the measurements [?]. It is assumed Gaussian-distributed with zero-mean and variance $\sigma_{s,m}^2(t_k)$.

- $\hat{\delta}_{n,m}(t_k)$ is an estimate of a pseudo inter agent distance between the terrestrial agents m and n

$$\hat{\delta}_{n,m}(t_k) = \|\mathbf{x}_n(t_k) - \mathbf{x}_m(t_k)\| + b_{n,m}(t_k) + \nu_{n,m}(t_k) \quad (4)$$

where $b_{n,m}(t_k)$ is a combination of the clock biases of the two agents and $\nu_{n,m}(t_k)$ is the noise of the measurements. For simplicity, as for the first class, it is assumed Gaussian-distributed with zero-mean and variance $\sigma_{n,m}^2(t_k)$ but its distribution can vary according to the range computation methods (i.e. single difference, double difference, raw pseudorange ranging) [?].

Let consider multiple ranges are expected to be obtained for each class assuming that measurements coming from the same class are independent. According to this assumption their error covariance matrices are diagonal and defined as $R_\rho(t_k) = \mathbf{E}[\boldsymbol{\rho}(t_k)\boldsymbol{\rho}(t_k)^T]$ and $R_\delta(t_k) = \mathbf{E}[\boldsymbol{\delta}(t_k)\boldsymbol{\delta}(t_k)^T]$ where $\boldsymbol{\rho}(t_k)$ and $\boldsymbol{\delta}(t_k)$ are generic *measurements vectors* composed by a set of S and N range measurements from each class, respectively. A hybrid positioning solution combines $\boldsymbol{\rho}(t_k)$ and $\boldsymbol{\delta}(t_k)$ in a *hybrid measurements vector*,

$$\boldsymbol{\mu}_m(t_k) = \begin{bmatrix} \boldsymbol{\rho}_m(t_k) & \boldsymbol{\delta}_m(t_k) \end{bmatrix}^T \quad (5)$$

whose *measurements noise covariance matrix* is hence defined as

$$R_{\boldsymbol{\mu}}(t_k) = \begin{bmatrix} R_\delta(t_k) & R_{\delta\rho}(t_k) \\ R_{\rho\delta}(t_k) & R_\rho(t_k) \end{bmatrix} \quad (6)$$

where the sub-matrices $R_{\rho\delta}(t_k) = R_{\delta\rho}(t_k) = \mathbf{0}$ if and only if terrestrial ranges are obtained independently from satellite-ranges already considered in $\boldsymbol{\mu}(t_k)$. This specific condition is satisfied for example in hybrid positioning with ranging sensors [?] while in this study this restrictive assumption is relaxed and $R_{\boldsymbol{\mu}}$, in (6), is not strictly a diagonal matrix.

III. FIM COMPUTATION IN LMS ESTIMATION

In the first part of this work, the estimations of the position is obtained by means of a LMS approach, which is a Best Linear Unbiased Estimator (BLUE) for Gaussian inputs [?]. It is largely used for the solution of the trilateration problem in positioning and navigation [?], besides being the usual initialization step of several navigation algorithms. Given a linearization point, \mathbf{x}_0 , the positioning solution can be computed iteratively as $[\hat{\mathbf{x}}_m(t_k) \ \hat{b}_m(t_k)]^T = [\mathbf{x}_0 \ b_0]^T + [\Delta\hat{\mathbf{x}}_m(t_k) \ \Delta\hat{b}_m(t_k)]^T$ where the approximation point is updated with the estimated at the previous iteration up to the expected convergence of the solution. The incremental step can be solved according to

$$\begin{bmatrix} \Delta\hat{\mathbf{x}}(t_k) \\ \Delta\hat{b}(t_k) \end{bmatrix} = (H^T H)^{-1} H^T \Delta\boldsymbol{\mu}(t_k) \quad (7)$$

where $[H]_s = \begin{bmatrix} \frac{\mathbf{x}_s - \mathbf{x}_m}{\|\mathbf{x}_s - \mathbf{x}_m\|} & 1 \end{bmatrix} = \begin{bmatrix} \mathbf{h}_{s,m} & 1 \end{bmatrix}$ and $\mathbf{h}_{s,m}$ is the *unitary steering vector* pointing towards the s -th satellites. The positioning solution obtained at each time instant, $\mathbf{x}_m(t_k)$, is independent from the previous one, $\mathbf{x}_m(t_{k-1})$, thus no information about the system dynamics is exploited in the estimation. In the following, the CRLB for LMS with Gaussian

independent measurement variables is obtained and compared to the hybrid solution, H-LMS, in which biased, dependent, non-Gaussian terrestrial measurements are combined.

As in (1), in order to evaluate the FIM it is sufficient to compute the second order derivative of the logarithm of the likelihood w.r.t. the vector $\boldsymbol{\theta}(t_k)$, where $\boldsymbol{\theta}(t_k) = [\mathbf{x}_m(t_k) \ b_m(t_k)]^T$ for the positioning estimation. Assuming a high-stability local clock and in order to reduce the complexity of the analysis, the bias term, b_m , will be eventually dropped as it can be assumed compensated by previous solution estimations, $\hat{\boldsymbol{\theta}}(t_{k-1})$.

A. Fisher Information Matrix for satellite only contributions

In the following derivation, time index is dropped for readability reasons. The theoretical log-likelihood for a Gaussian random variable is defined as

$$\mathcal{L}(\boldsymbol{\theta}, \rho, \sigma_i) = \sum_{i=1}^n \log \left(\frac{1}{\sqrt{2\pi}\sigma_i} \right) - \frac{(\mathbf{x} - \boldsymbol{\theta})^2}{2\sigma_i^2}. \quad (8)$$

Consequently, the log likelihood for a Gaussian pseudorange measured from a generic satellite, s , is obtained as

$$\begin{aligned} \mathcal{L}(\mathbf{x}_m, r_{s,m}, \sigma_{s,m}) &= \log p(\hat{\rho}_{s,m} | x_m, b_m) \\ &= C - \frac{|\hat{\rho}_{s,m} - ||\mathbf{x}_s - \mathbf{x}_m|| - b_m|^2}{2\sigma_{s,m}^2} \end{aligned} \quad (9)$$

where C is the constant term resulting from the first term of the summation in (8). As shown in [?], the Fisher Information matrix is computed as

$$F_m = -\mathbf{E} \left\{ H_m \left(\sum_s^{S_m} \mathcal{L}(\mathbf{x}_m, r_{s,m}, \sigma_{s,m}) \right) \right\} \quad (10)$$

where H_m is the Hessian operator of the second order partial derivatives and S_m is the cardinality of the set of satellites visible for the m -th user. The FIM is hence defined as

$$F_m = \begin{bmatrix} F_{\mathbf{x}_m} & \mathbf{f}_{x_m, b_m} \\ \mathbf{f}_{x_m, b_m}^T & F_{b_m} \end{bmatrix} \quad (11)$$

where each submatrix can be computed as

$$F_{\mathbf{x}_m} = \sum_{s \in S_m} \frac{1}{\sigma_{s,m}^2} \mathbf{h}_{s,m} \mathbf{h}_{s,m}^T \quad (12)$$

$$F_{b_m} = \sum_{s \in S_m} \frac{1}{\sigma_{s,m}^2} \quad (13)$$

$$\mathbf{f}_{\mathbf{x}_m, b_m}^T = \sum_{s \in S_m} -\frac{1}{\sigma_{s,m}^2} \mathbf{h}_{s,m}. \quad (14)$$

B. Fisher Information Matrix for cooperative contributions

For the sake of simplicity, the bias-free terrestrial range, $\hat{d}_{n,m}(t_k) = \hat{\delta}_{n,m}(t_k) - b_{n,m}(t_k)$, is obtained by means of the Inter-Agent Range (IAR) technique [?], [?] here recalled as

$$\hat{I}_{n,m}^s = \sqrt{\hat{r}_{s,m}^2 + \hat{r}_{s,n}^2 - 2\hat{r}_{s,n}\hat{r}_{s,m}(\mathbf{h}_{s,m} \cdot \mathbf{h}_{s,n})} \quad (15)$$

where $\hat{r}_{s,m} = \hat{\rho}_{s,m} - b_m$ and $\hat{r}_{s,n} = \hat{\rho}_{s,n} - b_n$. Given multiple shareable satellites between the two collaborating agents, the distance $d_{n,m}$ can be estimated as the weighted average of the single IAR contributions

$$\hat{d}_{n,m} = \sum_{s=1}^S w_s \hat{I}_{n,m}^s \quad (16)$$

where w_s terms are the weights attributed to each measurement according to its variance. It is worth to clarify that even considering i.i.d. satellite range estimates, the variance of each IAR contribution varies according to the geometry of the collaborating agents [?]. Furthermore, Although it has been shown that IAR is characterized by a Gaussian-like distribution, its statistics is very sensitive to the geometrical conditions [?]. By neglecting on purpose this peculiar behaviour, the same approach discussed for the evaluation of the FIM about satellite range measurements is applied to the likelihood defined for derived range measurements, such that

$$\log p\left(\hat{d}_{n,m}|x_m\right)=C-\frac{\left|\hat{d}_{n,m}-\left|\mathbf{x}_n-\mathbf{x}_m\right|-b_{n,m}\right|^2}{2\sigma_{n,m}^2}. \quad (17)$$

Actually, the likelihood of (16) is approximated by supposing the statistical identity between (15) and a Gaussian distributed distance measurement between the agents. Equation (10) is hence applied to (17) neglecting any dependency with respect to the other measurements. Eventually, the FIM for the hybrid system is computed according to (11). It has to be remarked that the CRLB of the hybrid solution is used only as an estimation of the variance of the hybrid position estimate and not as a lower bound, since the considered likelihoods cannot take into account inter-measurements correlation, measurement biases and potential non-Gaussian behaviour.

In the example shown in Figure 1, given a pre-defined trajectory, the value of the trace of the inverse of the FIM computed along the trajectory is expected to identify the profitable time instants in which cooperative approach guarantees improved precision w.r.t. GNSS standalone positioning.

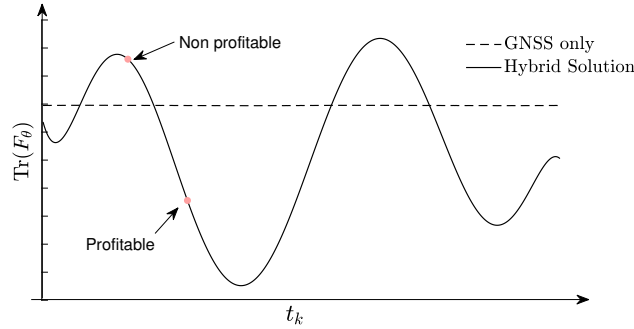


Fig. 1: Example of theoretical computation of satellite-based positioning CRLB vs. hybrid positioning CRLB for a dynamic trajectory.

The higher dynamic of the hybrid CRLB in Figure 1 is due to the higher variations in the relative position of the terrestrial agents w.r.t. the low variations w.r.t. the satellites. The profitability of the hybridization is hence defined as the percentage of time in which (2) is satisfied for the hybrid estimator.

The metric is evaluated from (2), as the ratio of the time instants t_k in which the condition

$$\text{Tr}\left([F_{\text{H-LMS},\mathbf{x}}(t_k)]^{-1}\right) < \text{Tr}\left([F_{\text{LMS},\mathbf{x}}(t_k)]^{-1}\right) \quad (18)$$

is satisfied w.r.t. the overall simulation time. The *profitability percentage* of the methods will be referred to as τ_{SIM} (obtained by means of Monte Carlo simulations) and τ_{CRLB} (obtained from the theoretical definition) to describe the precision improvement of H-LMS computed from the numerical simulation and from CRLB, respectively, with the aim of assessing the use of the theoretical metric as an index of effectiveness.

IV. FIM COMPUTATION IN NON-LINEAR SYSTEMS ESTIMATION

Given that a reduced uncertainty about the computed position is not useful for real-time applications it is instead intuitive that a refinement of the position at a given instant t_k by means of the proposed integration scheme could lead to an improved estimate of the position at the following instant t_{k+1} . The update step provided by Bayesian estimation algorithms can benefit from this early refinement, such as in the case of the proposed modified EKF. The EKF is a Bayesian estimator widely used in the estimation of system dynamics due to the capability of constraining the positioning solution according to a model of the dynamics of the motion and exploiting the relationship of the state at the previous instant with the current state. Such an estimation typically outperforms LMS estimation both in terms of accuracy and precision. Furthermore, EKF is a non-linear extension of the plain KF, thus it allows to integrate non-linear measurements through a linearized model which links state and measurements such as for LMS estimation. Additional details about EKF fundamentals and implementation are left to the reader and they can be found in [?].

A. CRLB for deterministic non-linear systems

The CRLB for dynamic systems is modelled by non-linear time-varying state vector differential equations with deterministic inputs and non-linear time-varying observations on the state variables, corrupted by additive Gaussian white noise [?]. It has been demonstrated that FIM propagates according to the error covariance matrix for an EKF linearized w.r.t. the true trajectory. For this reason, the FIM can be computed as

$$F_k = (\Phi_{k-1}^{-1})^T F_{k-1} \Phi_{k-1}^{-1} + H_k^T R_k^{-1} H_k \quad (19)$$

where Φ_k denotes the state transition matrix at the time t_k . For simplicity, the process noise is omitted in this analysis but it can be taken into account by considering the Posterior CRLB, defined in [?]. Provided that the true trajectory is not available, the Jacobian matrix H_k cannot be built w.r.t. the true position at the time t_k . The matrix can be replaced by the Jacobian matrix defined for the current position estimate. An approximation of the CRLB can hence be pursued by analysing the amount of information provided by the measurements set w.r.t. the last available estimated position. The suggested approximation is oriented to the effective integration of collaborative measurements only when they improve the localization performance but it could not be reliable in case of a degraded quality of the measurements.

V. SIMULATION ANALYSIS

The numerical simulation scheme presented in this Section aims at analysing the impact on the positioning algorithm of the target agent which integrates correlated satellite and dependent terrestrial range measurements.

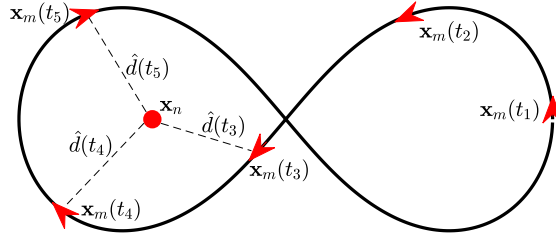


Fig. 2: Example of a path based on a Bernoulli lemniscate of 1046.7 m travelled at an average speed of 26.15 m/s. The dashed lines show the auxiliary range measurements provided according to (15) at different time instants.

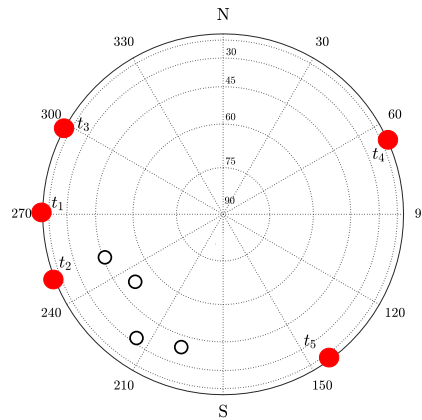


Fig. 3: Skyplot of the azimuth, ϕ , and elevation, α , of the satellites (white dots) and the aiding agent (red dots) w.r.t. the position of the target agent at given time instants.

The example reported in this paper has been chosen to easily identify profitable and not-profitable integration time spans. A single aiding agent is selected and a set of four satellites is generated by simulating limited visibility conditions of the sky (i.e. azimuth $\phi \in \{\pi, \frac{3}{2}\pi\}$ and elevation $\alpha \in \{\frac{\pi}{24}, \frac{\pi}{2}\}$). The target agent moves following the Bernoulli path in Figure 2 while the aiding agent position, \mathbf{x}_n , is assumed static for any t_k . In the considered scenario both the agents estimate their positions relying on the set of satellites depicted in Figure 3. The target agent is designed to exploit the IAR information obtained at each time instant, t_k , through the collaboration with the aiding agent.

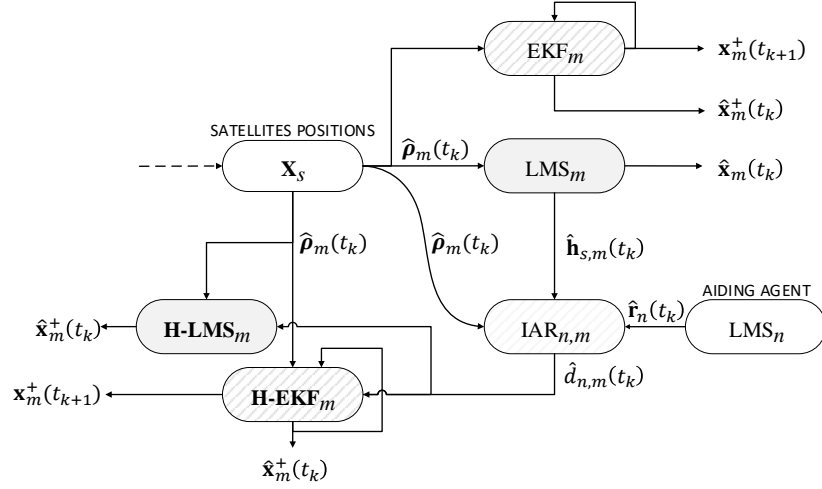


Fig. 4: Block scheme of numerical simulations. The outputs of the LMS and EKF blocks were compared to the respective hybrid versions to assess the positioning performance. \mathbf{X}_S indicates the positions of the visible satellites.

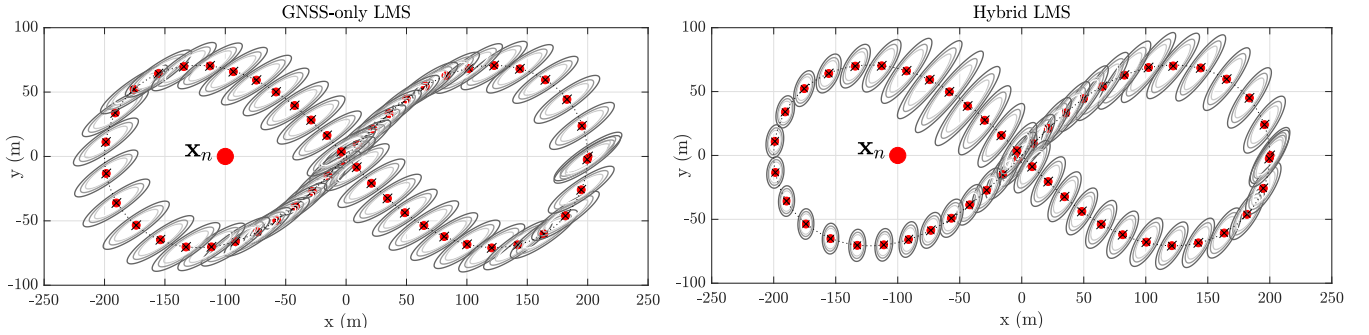


Fig. 5: Estimated positioning solutions according to the scenario in Figure 2. The information ellipses describe the horizontal standard deviation at 90%, 99% and 99.9% of confidence interval, obtained from the eigenvalues of the matrix \mathbf{P}_x in a subset of time instants, t_k . Results from a Monte Carlo simulation with parameters $W = 10000$, $\sigma_{s,m} = 1$, $\max(d_{n,m}) = 300$ m.

As depicted in the scheme in Figure 4, the GNSS-only positioning, referred to as LMS or EKF, is first performed to obtain $\hat{\mathbf{x}}_m(t_k)$, then navigation data are used to determine collaborative ranges $\hat{d}_{n,m}(t_k)$ which are integrated in a further hybrid positioning computation, named H-LMS or H-EKF, to refine the previous outcome, hereafter referred to $\hat{\mathbf{x}}_m^+(t_k)$.

The axial standard deviations were measured from the numerical simulation and, in parallel, estimated through the CRLB (1).

In the following, the analysis is based on a Monte Carlo simulation by consider W realizations of the trajectory of the moving agent. Pseudorange measurements are the only random variables responsible of variations among the trials. The IAR measurements are expected to vary along with the time, t_k , while satellites are assumed static to limit the variability of the scenario. The measurement and the positioning estimation are performed for each run at the same time instant, t_k .

The error covariance matrix of the positioning solution is estimated as

$$\hat{\mathbf{P}}_x(t_k) = \frac{1}{W-1} \sum_{w=1}^W (\hat{\mathbf{x}}_w(t_k) - \mu(t_k)) (\hat{\mathbf{x}}_w(t_k) - \mu(t_k))^T \quad (20)$$

In the following, the horizontal components of (20) are plotted as *information ellipses* [?] according to the eigenvalues of the position error covariance matrix. The positioning bias is computed as the mean error w.r.t. to true position of the target agent

$$\hat{\xi}_{\mathbf{x}}(t_k) = \frac{1}{W-1} \sum_{w=1}^W (\hat{\mathbf{x}}_w - \mathbf{x}(t_k)). \quad (21)$$

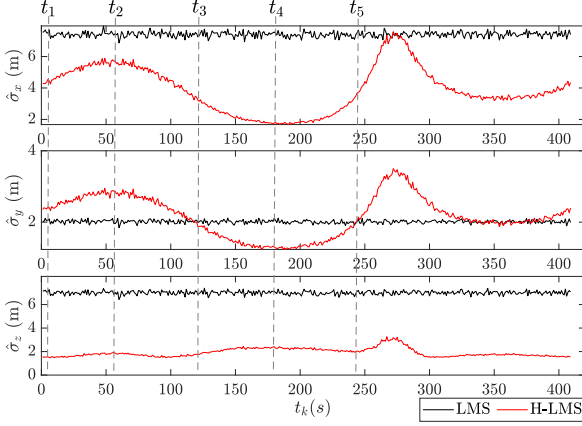
In order to observe the correlation among the measurements involved in the hybrid estimation of the position, the *Pearson correlation coefficients* of the measurements vector are computed as

$$C(\rho_1(t_k), \rho_2(t_k)) = \frac{\text{cov}[\rho_1(t_k), \rho_2(t_k)]}{\sigma_{\rho_1(t_k)} \sigma_{\rho_2(t_k)}}. \quad (22)$$

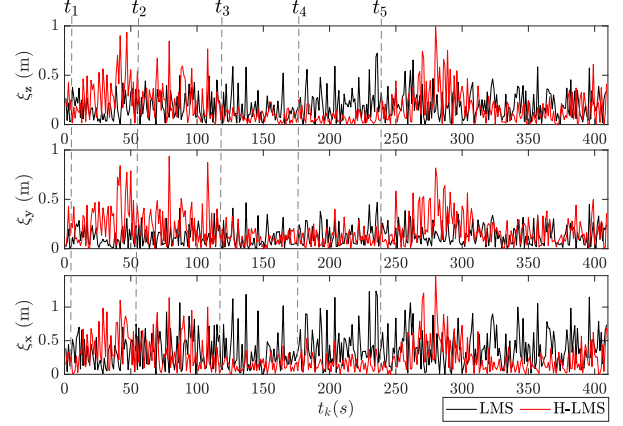
VI. NUMERICAL RESULTS IN HYBRID POSITIONING

A. H-LMS performance

In this section, results from the aforementioned Bernoullian trajectory are presented. They address the determination of the profitability of the H-LMS by comparing the values obtained from numerical simulation and theoretical CRLB. A set of elementary trajectories is then tested to extend the analysis to a wider range of geometrical conditions for the target agent.



(a) Axial standard deviations estimated according to (20).



(b) Axial biases estimated according to (21).

Fig. 6: Statistical analysis of simulation biases and standard deviations provided by LMS/H-LMS estimation of the position.

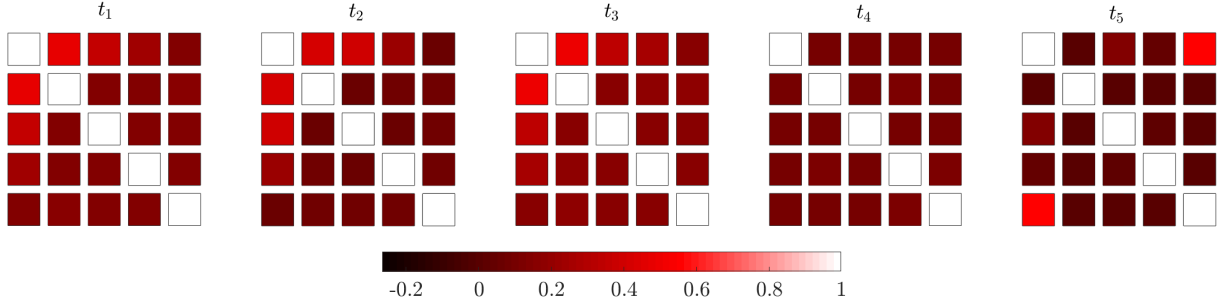


Fig. 7: Graphical representation of the matrix of Pearson correlation coefficients (22) computed for the measurement error covariance \mathbf{R}_μ , and observed at different time instants t_k where $k \in \{1, 5\}$.

B. Bernoullian trajectory

The results presented in this subsection are referred to the example of collaborative scenario depicted in Figure 2 and obtained by means of a Monte Carlo simulation using $W = 10000$ trials for each time instants t_k . In Figure 5, the positioning solution of the LMS (left) and H-LMS (right) are presented. The information ellipses shows a remarkable difference between the two approaches in terms of error covariance matrix of the positioning solution. The most significant improvement can be observed between the time instants t_3 and t_5 . The time series of axial biases and standard deviations are reported in Figure 6a and Figure 6b, respectively. It is evident from the plots that the hybrid solution integrating IAR measurements reduces the uncertainty in some specific portion of the path. It is worth to notice that both the metrics show a higher dynamics for the hybrid solution due to the fast variations in the relative positions of the agents w.r.t. the slower change rate of the satellite-to-target geometry, as expected.

By considering the standard deviation behaviour depicted in Figure 6a, it is remarkable that on y -axis the aforementioned improvement is still well visible between t_3 and t_5 when the collaborating agent is in azimuthal opposition w.r.t. the satellites. The z -axis is instead less sensitive to the dynamics of the agents since their relative elevation does not vary along the trajectory. As shown in 6b, also the bias presents a similar behaviour, showing improved performance according to the same favourable position of the collaborating agent, \mathbf{x}_n .

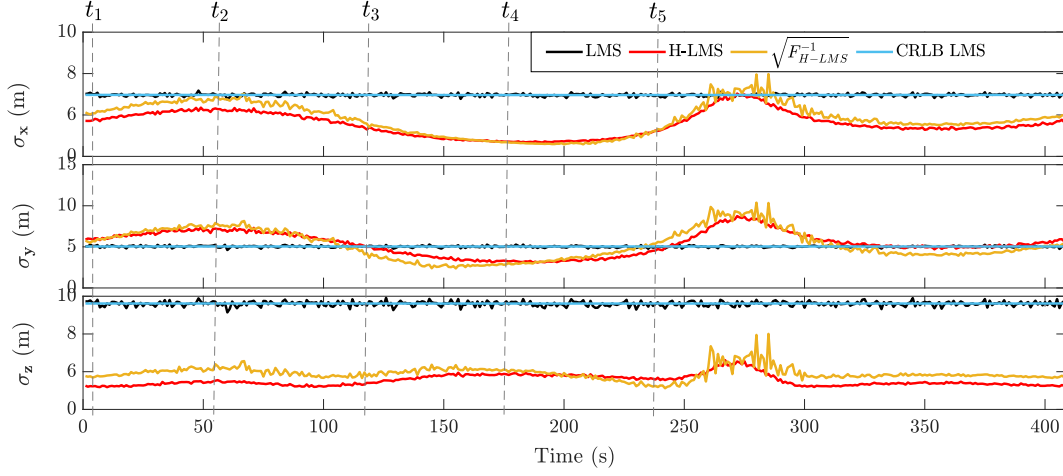


Fig. 8: Comparison of measured axial standard deviations from the CRLB for LMS positioning and estimated standard deviations obtained through H-LMS by Monte Carlo simulations.

The plots in Figure 7 shows the Pearson correlation coefficients (22) of the measurements at the different time instants t_k . The first row and column of each matrix indicates the correlation coefficients related to the dependent IAR measurement. It can be observed that in correspondence to t_4 , a-posteriori identified as the most beneficial time-instant for cooperation, a very low correlation can be observed among the measurements. To observe the benefits of H-LMS from the theoretical point of view, Figure 8 shows the comparison of the standard deviation computed via numerical simulation and the estimated ones obtained for the CRLB estimation of both the solutions. While the quantities match perfectly in the case of LMS, CRLB is not accurate for H-LMS due the nature of the estimator including the IAR measurements. In correspondence of t_4 , where the uncorrelation has been observed among terrestrial and satellite ranges, numerical values and theoretical estimations tend to match. The profitability percentage in terms of horizontal precision of the H-LMS is evaluated computing the percentage of the time in which the trace of the covariance matrices and the CRLB of the H-LMS are lower than the respective values from the LMS. As anticipated in III, the profitability percentage computed by means of estimated CRLBs is 91.93% which is remarkably close to the value obtained from simulated data 89.73%.

C. Other trajectories

The same scenario of satellites and aiding agent locations is used on a set of trajectories to extend the analysis. All the trajectories are centered around the origin of the simulated scenario. As shown in Table I, the evaluation of the profitability

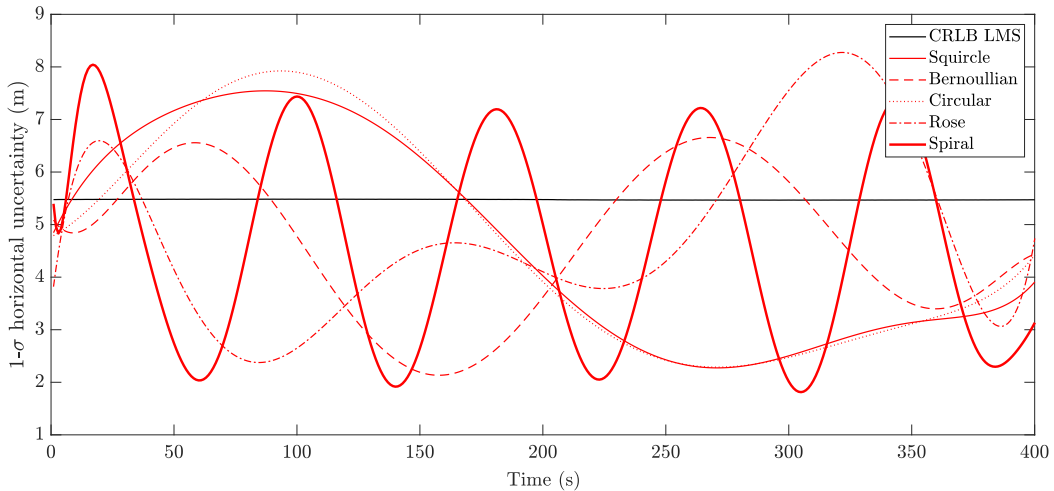


Fig. 9: Square root of the horizontal trace of F_{H-LMS}^{-1} computed for H-LMS in different elementary geometrical trajectories vs. horizontal CRLB computed for LMS.

TABLE I: Comparison of profitability of H-LMS for other elementary geometrical trajectories

Trajectory Shape	τ_{SIM}	τ_{CRLB}	MSE (m)
Squircle	72.21%	81.90%	0.26
Circular	73.11%	79.46%	0.21
Rose lemniscate	74.57%	77.50%	0.16
Archimedeia Spiral	75.41%	80.67%	0.13
Bernoullian lemniscate	89.73%	91.93%	0.15

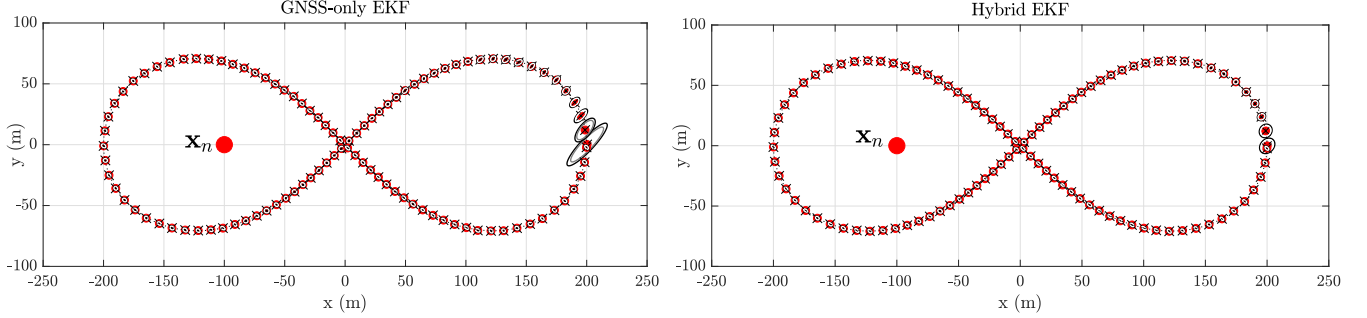


Fig. 10: Estimated EKF and H-EKF positioning solutions according to the scenario depicted in Figure 2. The information ellipses describe the horizontal standard deviation at 90%, 99% and 99.9% confidence intervals, obtained from the eigenvalues of the matrix $P_{\mathbf{x}}$ in a subset of time instants, t_k . Results from a Monte Carlo simulation with parameters $W = 10000$, $\sigma_{s,m} = 1$, $\max(d_{n,m}) = 300$ m.

percentage, τ_{CRLB} , through the proposed estimation is more conservative w.r.t. the actual simulation results. Furthermore, the Mean Square Error (MSE) computed along the trajectory between simulated and theoretical value is almost negligible for all the tested trajectories. Figure 9 summarizes the horizontal values of the theoretical CRLB computed for the H-LMS using the different geometrical trajectories. The values are compared to the CRLB computed for LMS which is almost constant along all the trajectories due to the considerable distance of the satellites from the target at each t_k .

D. H-EKF performance

Figure 10 shows the same Bernoullian path presented in Figure 5 along with the estimated position and associated information ellipses obtained by means of EKF-based positioning. Differently from the LMS-based solutions, the benefits of the hybridization are less evident in the EKF-based navigation algorithm. However it is still remarkable to notice a faster convergence of the covariance at the beginning of the motion.

The CRLB defined for EKF is less sensitive to the geometry of the system as shown in the theoretical limit computation in Figure 11. This is partially due to the convergence of the covariance along the trajectory path which masks the dynamics of the

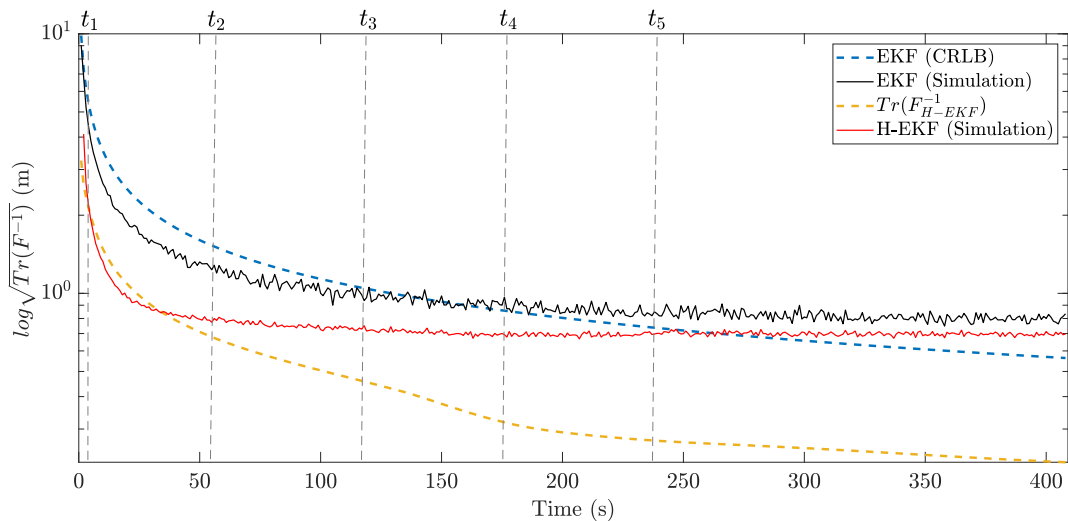


Fig. 11: CRLB computed for EKF and H-EKF compared to the statistical values of the trace of the error covariance of the position obtained from the Monte Carlo simulation. The ordinate axis is logarithmic scale for improved readability.

CRLB. However, the example shows that the theoretical advantage between EKF and H-EKF is remarkable. It can be observed that as far as the trace converges, the information carried by collaborative measurements becomes less relevant, differently from what we expect in theory. It has to be noticed that approaching the time instant t_4 , the CRLB for H-LMS shows a faster decrement which matches the analysis performed for the H-LMS algorithm while the same behaviour is not evident in the experimental values. The profitability analysis of the integration of auxiliary measurements in EKF scheme provided values of 100% for all the tested trajectories shown in Table I but due the peculiar considerations made for the EKF, the comparison between theoretical and experimental values is not worthy to be reported.

VII. CONCLUSIONS

The hybridization of GNSS-based collaborative terrestrial ranges and satellite-based measurements can increase the performance of standalone satellite positioning similarly to independent terrestrial contributions. In particular, when the geometry of the visible satellites is poor, as investigated in Section VI, the additional information provided by collaborating agents mostly compensates for a severe dilution of precision.

The non-linear formula employed for the IAR computation between the two agents provides an example of non-independent non-Gaussian measurements whose distribution does not correspond with the likelihood employed in LMS and EKF and used to derive the respective CRLBs (17). In these cases the measured covariance can be even lower than the CRLB as shown in the examples discussed in Section VI. This results are indeed supported by the theory related to biased estimators and stability conditions of the CRLB.

The relevance of the presented results is threefold. On one side it has been shown that non-independent measurements can bring information to the positioning estimation. Furthermore, the simplistic usage of the likelihood function for Gaussian distributed variables with IAR measurements confirmed that their distribution is not always Gaussian thus leading to overoptimistic and over-pessimistic outcomes. This mainly depends on the quality of pseudoranges and on the geometry of the collaborating agents. In the end, the advantage of the proposed hybrid positioning strictly depends on the combined geometry of the terrestrial ranging information and satellites constellation. Summarizing, the used likelihoods definition and the related CRLB for the hybridization of cooperative range measurements can be used as an approximation to determine whether inter-agent collaboration can improve navigation and positioning performances. Further work addressing realistic trajectories and error models can be found in [?].



Alex Minetto received the M.Sc. in telecommunications engineering (Information Theory and Signal Processing Applications) from Politecnico di Torino, Italy, in 2015. He is currently a PhD candidate at the Department of Electronics and Telecommunications of Politecnico di Torino within the Navigation Signal Analysis and Simulation (NavSAS) research group. He was an intern at the European Organization for the Exploitation of Meteorological Satellites (EUMETSAT) in Darmstadt (Germany), addressing the development of a new precise detection algorithm for radar pulses sent from Metop satellites during their calibration campaign. His research interests include information theory, advanced signal processing, Global Navigation Satellite System (GNSS), and collaborative positioning.